Available online at www.sciencedirect.com
SCIENCE DIRECT®
Optics Communications 246 (2005) 495–503
OPTICS COMMUNICATIONS
www.elsevier.com/locate/optcom

Analysis on femtosecond pulses generated by passively mode-locked lasers with higher-order effects

Lijun Song *, Xiaojuan Shi, Wenrui Xue, Zhonghao Li, Guosheng Zhou

The State Key Subject of Optics, State Key Laboratory of Quantum Optics and Quantum Optics Devices, Department of Electronics and Information Technology, Shanxi University, No. 36 Wucheng Road, Taiyuan, Shanxi, 030006, China

Received 3 July 2004; received in revised form 10 October 2004; accepted 4 November 2004

Abstract

A theoretical model for passively mode-locked lasers is presented, in which the higher-order effects, such as third-order dispersion, nonlinear dispersion, and self-frequency shift arising from stimulated Raman scattering, and a fast as well as a slow saburable absorber responses are taken into account. An exact soliton-like solution is obtained under a definite parameter conditions and its stability is also analyzed numerically under small perturbations in amplitude, chirp and white noise. The results indicate that the pulses can be stable under a finite perturbation and become identical to the exact solution after a distance of evolution. In addition, we have also found that a quite arbitrary initial Gaussian pulse can converge to the exact solution after a distance of evolution.

PACS: 42.55.P,R; 42.65.R; 42.65.T
Keywords: Solid-state laser; Ultra-short pulse; Semiconductor saturable absorber

1. Introduction

Passively mode-locked solid-state lasers for short pulse applications experience a renaissance with the invention of the semiconductor saturable absorber mirror (SESAM) [1] and have been further investigated experimentally [2–5] and theoretically [6–10]. Recent reports of ultrashort pulse solid-state lasers present that passively mode-locked techniques have led to the capability to generate pulses in the sub-10 fs regime [11–14]. Ultrashort pulse generation in solid-state laser system makes use of a variety of schemes, where the use of a SESAM has been recognized as a practical way to obtain stable femtosecond pulses in cw-pumped self-starting lasers [3,4]. The uses of semiconductor as saturable absorber are attractive because they are inexpensive and compact; the

* Corresponding author. Tel.: +863517016058; fax: +86351701433.
E-mail address: songlij@sxu.edu.cn (L. Song).

0030-4018/$ - see front matter © 2004 Elsevier B.V. All rights reserved.
doi:10.1016/j.optcom.2004.11.011

important operation parameters such as saturation intensity, spectral range of the bandgap, linear loss, and response time can be generally designed [15].

The theoretical investigations of passively mode-locked laser systems have been done by use of two almost opposite approaches. In the first approach, which is computational, one simulates the entire evolution of light within the laser, starting from noise. In the second one, which is analytical and first introduced by Haus [6], one uses an idealization in which the pulse evolution during a single pass through the laser is assumed to be small to obtain a simple equation. In 1998, Akhmediev et al. [10] have described pulses evolution of passively mode-locked lasers by a modified complex Ginzberg–Landau equation (CGLE), in which they take a fast as well as a slow saturable absorber responses into account. But for pulses, whose widths are shorter than 100-fs, several new processes, such as third-order dispersion (TOD), nonlinear dispersion, and self-frequency shift (SFS) arising from stimulated Raman scattering, become very important. Zhonghao Li et al. [9] have presented another model of laser pulses evolution with the higher-order terms taken into account.

As presented by Keller [16], passive mode-locking mechanisms can be well-explained by three fundamental models: slow saturable absorber mode-locking with dynamic gain saturation [6,17], fast saturable absorber mode-locking [18,19] and soliton mode-locking [20–22]. A typical example of the fast saturable absorber mode-locking is Kerr-lens mode-locking (KLM) [4], where an artificial fast saturable absorber is formed by the self-focusing that occurs inside the laser crystal. But the Kerr nonlinearity is usually not strong enough for the cw mode-locking process to self start. In order to initiate KLM, a separate starting mechanism, such as SESAM, is required. Otherwise, for soliton mode-locking, the absorber dynamics is also necessary to stabilize the soliton against the growth of background radiation, in which the pulse is completely shaped by soliton formation, i.e., the interplay between negative group-delay dispersion (GDD) and self-phase modulation (SPM). The main difference between KLM and soliton mode-locking can be found in the temporal behavior of the saturable absorber action. KLM is an artificial fast saturable absorber, whereas soliton mode-locking is based on a slow saturable absorber realized by the SESAM.

However, another case may be existed in experiments when the laser is difficult or problematic for KLM. The pulse formation is accomplished not only by the balance between GDD and SPM, but also by the interactions happened among TOD, higher-order nonlinearities, the fast and the slow saturable absorber responses. In this paper, we present a general theoretical model for passively mode-locked lasers, in which the higher-order effects and a fast as well as a slow saburable absorber response are taken into account. An exact analytical soliton-like solution is also obtained and its stability is analyzed numerically under small perturbations in amplitude, chirp and white noise. The results indicate that the pulse can be stable in a definite parameter range. It means that the combined balances among the higher-order effects, the slow and the fast saturable absorber responses can cause the generation of stable femtosecond soliton-like pulses. The evolution of a quite arbitrary initial Gaussian pulse shows that the Gaussian pulse can converge to the exact solution after a distance of evolution. The paper is organized as follows. In Section 2, we introduce the model and present soliton-like solution and their existence conditions. In Section 3, the characteristics of the solution pulse parameter are investigated. In Section 4, the stability of the solution and the evolution of an initial Gaussian pulse are analyzed numerically. We conclude the paper in Section 5.

2. Model and solutions

When both the saturable absorber responses and higher-order effects are all taken into account, the pulse evolution is governed by a higher-order modified complex Ginzberg–Landau equation, that is

$$\begin{aligned} E_z - \mathrm{i}\frac{D}{2}E_{\mathrm{tt}} - i|E|^2E &= [g(Q) + \chi|E|^2 - \delta_s(t)]E + \varepsilon E_{tt} + \lambda E_{ttt} \\ &\quad + \kappa(|E|^2E)_t + \mathrm{i}vE(|E|^2)_t, \end{aligned} \tag{1}$$

where z is the cavity round-trip number treated as a continuous variable, t is the retarded time, $E(z,t)$ is the normalized envelope of the optical field, D is the group-delay dispersion coefficient and $D = 1$ corresponds to anomalous dispersion, $g(Q)$ is the cavity gain, which depends on the total energy Q of the pulse in one round trip, and $\delta_s(t)$ is the loss, which includes the loss in the saturable absorber, χ is responsible for the effects of fast saturable absorption, ε stands for spectral filtering ($\varepsilon > 0$), λ represents the TOD, κ is the nonlinear dispersion term, which is responsible for self-steepening at the pulse edge, and the term with v is the nonlinear gradient which results from stimulated Raman scattering, which is usually responsible for the soliton self-frequency shift.

The gain term $g(Q)$ in Eq. (1) describes a gain medium with a recovery time T_L, which is much longer than the round-trip time of the cavity and which does not depend explicitly on t. It can be described by the rate equation [10]

$$\frac{\partial g(Q)}{\partial z} = -\frac{g(Q) - g_0}{T_L} - \frac{Q}{T_R E_L} g(Q), \tag{2}$$

where g_0 is the small-signal gain, $T_R = 1$ is the round-trip time, and E_L is the gain saturation energy. The value of $g(Q)$ decreases with increasing pulse energy, so within each round trip the pulse energy is limited.

When the recovery time of the saturable absorber T_1 is longer compared with the pulse width, the loss $\delta_s(t)$ can be approximated by the following formula [10]

$$\delta_s(t) = \delta_0 - \alpha_1 \int_{-\infty}^{t} |E|^2 \mathrm{d}t' + \alpha_2 \left(\int_{-\infty}^{t} |E|^2 \mathrm{d}t' \right)^2 + \cdots, \tag{3}$$

where δ_0 is the loss introduced by the absorber in equilibrium, and $\alpha_1 = \delta_0/E_A$, $\alpha_2 = \delta_0/E_A^2$, E_A is the saturation energy of the absorber. Substituting approximation (3) into Eq. (1), we obtain

$$\begin{aligned} E_z - \mathrm{i}\frac{D}{2}E_{tt} - \mathrm{i}|E|^2 E &= \delta E + \varepsilon E_{tt} + \chi |E|^2 E + \lambda E_{ttt} + \kappa (|E|^2 E)_t \\ &\quad + ivE(|E|^2)_t + \alpha_1 E \int_{-\infty}^{t} |E|^2 \mathrm{d}t' \\ &\quad - \alpha_2 E \left(\int_{-\infty}^{t} |E|^2 \mathrm{d}t' \right)^2, \end{aligned} \tag{4}$$

where $\delta = g - \delta_0$. We find that Eq. (4) has an exact soliton-like solution that moves with group velocity $1/V$:

$$E(t,z) = A_0 \operatorname{sec} h[\eta(t - Vz)]^{1+i\beta} \exp[\mathrm{i}(\Omega t - Kz)], \tag{5}$$

Here A_0, η, V, β, Ω, and K are the parameters described the amplitude, the inverse pulse width, inverse group velocity, chirp, frequency shift and phase shift of the pulse, respectively. By substituting Eq. (5) into Eq. (4), eight real algebraic equations for the free parameters are obtained. Their solution is:

$$\beta = -\frac{1}{3\kappa}\left(4v + \frac{27\kappa^2 - 16v^2}{R} - R\right), \tag{6}$$

$$\Omega = \frac{4b_1\lambda - Db_2\kappa - 6\beta\varepsilon\kappa}{2b_4\lambda\kappa}, \tag{7}$$

$$\eta = \frac{2\alpha_1 b_1 \lambda\kappa \pm \{4\alpha_1^2 b_1^2 \lambda^2 \kappa^2 + 4\kappa^2 b_8 [8\alpha_2 b_1^2 \lambda^2 + \beta\kappa^2 b_7 - \varepsilon b_1 \kappa^2]\}^{1/2}}{2[8\alpha_2 b_1^2 \lambda^2 + \beta\kappa^2 b_7 - \varepsilon b_1 \kappa^2]} \tag{8}$$

$$A_0 = \eta[2b_1\lambda/\kappa]^{1/2}, \tag{9}$$

$$K = -\frac{1}{2}[\eta^2 b_1 b_7 - \Omega^2 b_5 + 4\beta\varepsilon\eta^2], \tag{10}$$

$$V = \Omega b_6 - b_3\lambda\eta^2 - 2\varepsilon\Omega/\beta, \tag{11}$$

where

$$R = [216\kappa^2 v - 64v^3 + 3\sqrt{3}(729\kappa^6 + 432\kappa^4 v^2 - 256\kappa^2 v^4)^{1/2}]^{1/3}, \tag{12}$$

and

$$b_1 = 1 - \beta^2,\ b_2 = 2 - \beta^2,$$
$$b_3 = 3 - \beta^2,\ b_4 = 4 - \beta^2,$$

$$b_5 = D + 2\lambda\Omega,\ b_6 = D + 3\lambda\Omega,$$
$$b_7 = D + 6\lambda\Omega,\ b_8 = \delta - \varepsilon\Omega^2. \tag{13}$$

In addition, the chirp parameter β together with parameters δ, ε, χ, λ, μ, ν, α_1 and α_2 must satisfy the compatibility conditions as follows:

$$4\alpha_2\beta b_1^2\eta\lambda^2 - \alpha_1\beta\lambda\kappa b_1 = \kappa^2(1+\beta^2)(\beta\eta^2\lambda + \varepsilon\Omega), \tag{14}$$

$$4b_1\lambda(2\alpha_2 b_1\lambda + \kappa\chi) = \kappa^2(2b_2\varepsilon - 3\beta b_7). \tag{15}$$

We note that the quantity under square root sign in Eq. (12) defines a relationship between the self-steepening term κ and the SFS term ν, which is $\kappa^2 \geqslant 0.36624\nu^2$. If λ, κ and ν are all negative, the range of chirp parameter β can be determined by Eq. (9) and $b_1 = 1-\beta^2$, $\beta \in [-1, 1]$, which ensures A_0 is real. More than that the quantity under the square root sign in η (Eq. (8)) must be positive, that is:

$$4\alpha_1^2 b_1^2\lambda^2\kappa^2 + 4\kappa^2 b_8[8\alpha_2 b_1^2\lambda^2 + \beta\kappa^2 b_7 - \varepsilon b_1\kappa^2] \geqslant 0. \tag{16}$$

From the inequality (16), we can obtain the parameter regions where the soliton-like solution exists. Regions of the linear loss (or gain) δ and chirp parameter β are shown in Fig. 1(a) for $\varepsilon = 0.13$, $\lambda = -0.02$, $\kappa = -0.03804$, $\nu = -0.01$, $\alpha_1 = 0.02$, $\alpha_2 = 0.01$ and $D = 1$. The region is divided into two subregions: the first has negative loss and arbitrary chirp when $\beta \leqslant 0.107$; in the second, the pulse exists inside a narrow domain of δ and β.

When the self-frequency shift $\nu = 0$, $\kappa \neq 0$ and $D = 1$, we can obtain from the original eight real algebraic equations that $\beta = 0$, $\Omega = 0$ and the compatibility conditions of $2\lambda = \kappa$, $\alpha_2 + \chi = 2\varepsilon$. That is to say, when the self-frequency shift arising from stimulated Raman scattering is not taken into account, the soliton solution without chirp and frequency shift can be generated under the balances of various effects presented in the equation. The corresponding region, where the solution exists, is shown in Fig. 1(b). Here, we will emphasize the first compatibility condition shown above, $2\lambda = \kappa$, which presents the interplay between the third-order dispersion and the self-steepening term

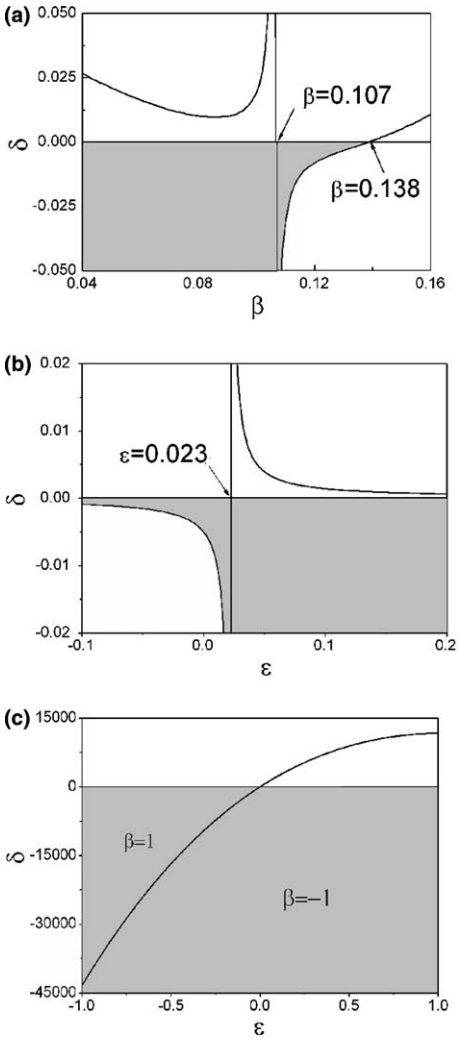

Fig. 1. (a) Space of the linear loss (or gain) δ and chirp parameter β in which the solution exists. The shaded areas are defined by inequality (16); (b) Space of the linear loss (or gain) δ and ε for $\nu = 0$ and $\kappa \neq 0$; (c) Space of the linear loss (or gain) δ and ε for $\kappa = 0$ and $\nu \neq 0$.

when $\nu = 0$. When $\alpha_2 = 0$, the interplay between the spectral filtering term and the fast saturable absorber can be obtained from the second compatibility condition $\chi = 2\varepsilon$.

When the self-steepening term is not taken into account ($\kappa = 0$), there will be $\beta = 1$ or -1. That is, the soliton-like pulses with stationary chirp are generated under the balances among the third-order dispersion, the self-frequency shift, and the

other effects presented in the equation. The corresponding region is shown in Fig. 1(c). If the third-order dispersion parameter is equal to zero, we can obtain from the original eight real algebraic equations that $v = 0$ and $\kappa = 0$. Eq. (4) becomes the same as that presented in [10]. This may tell us that interactions, which happened among the higher-order effects, exist and play an important role when pulses, whose width is shorter than 100-fs, are analyzed.

3. Discussion

It is well known that various effects, such as third-order dispersion or the action of a slow saturable absorber, tend to make the pulse asymmetric when only one of them works. When together with other effects, such as the nonlinear dispersion term and the nonlinear gradient term, the interaction among them may keep the pulse in symmetric shape of the temporal intensity profile. The symmetric pulses were obtained both experimentally [3,4] and theoretically [8,9] when the third-order dispersion, nonlinear dispersion, nonlinear gradient, and sabturable absorber response were taken into account. As specified by the two signs in the expression of the inverse pulse width η (Eq. (8)), there are two branches of the solution. For $\eta = \eta_-$ the solution amplitude approaches to zero with increasing of the loss δ (Fig. 2(a)) and α_1 (Fig. 2(b)). While for $\eta = \eta_+$ the solution amplitude is blowing up with increasing of δ and α_1 (see the inlays in Fig. 2). So the solution for $\eta = \eta_+$ is not stable and we shall not consider it further.

As an example, the soliton profile of the solution and the total gain (or loss) curve $\delta(t)$ are shown in Fig. 3(a) for the parameter values used in Fig. 1. As can be seen from Fig. 3(a), the solution is tightly related with the gradient of the total gain (or loss) curve

$$\delta(t) = \delta + \chi|E|^2 + \alpha_1 \int_{-\infty}^{t} |E|^2 \mathrm{d}t' - \alpha_2 \left(\int_{-\infty}^{t} |E|^2 \mathrm{d}t' \right)^2. \tag{17}$$

Clearly, the background is unstable if there is positive gain on one or both sides of the pulse. A realistic choice is therefore negative δ, as this causes the total gain to be negative on both sides of the pulse, as shown in Fig. 3. A net gain window is formed by the responses of the slow and the fast saturable absorber. So the growth of the continuum and the vibrations on both sides of the pulse are suppressed and narrower pulses are generated. At the limit case of $\alpha_1 \to 0$, which is corresponds to the mode-locking due to SESAM, the profile of the total gain (or loss) for $\alpha_1 = 0$ and $\alpha_2 = 0.001$ are shown in Fig. 3(b). A net gain window is also formed by the quadratic in energy term of slow loss variation and the fast saturable absorption. And the quadratic term plays an important role in the generation of stable pulses.

We have also investigated the dependences of the pulse widths on the parameters TOD λ, the nonlinear absorption α_1, chirp β, and frequency

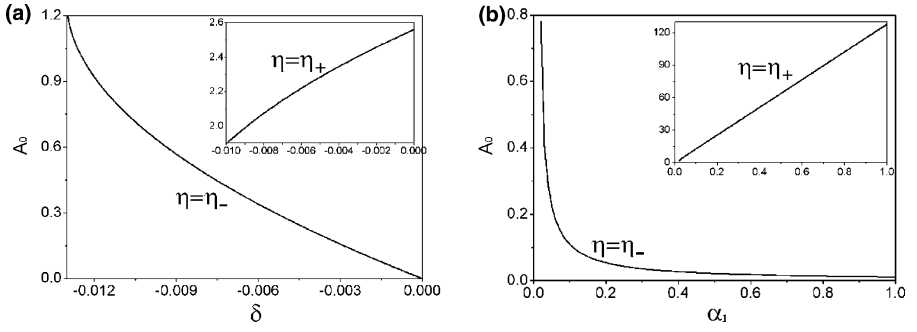

Fig. 2. Dependence of the pulse amplitude A_0 on (a) δ and (b) α_1 for η_+ and η_-.

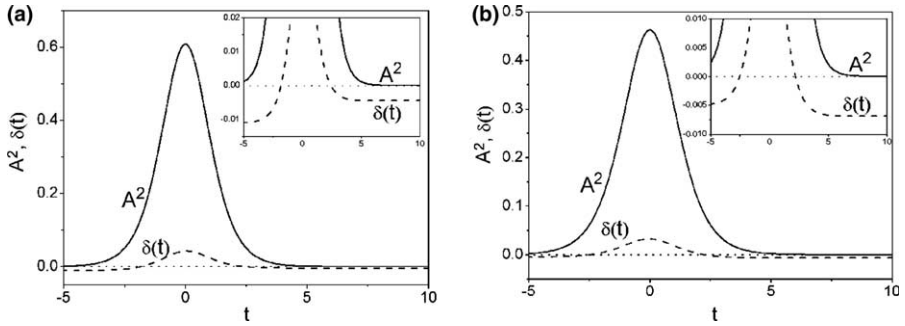

Fig. 3. Pulse profile (solid curve) and loss curve $\delta(t)$ (dashed curve) for $\varepsilon = 0.13$, $\lambda = -0.02$, $v = -0.01$, $\kappa = -0.03804$ and $D = 1$, (a) $\alpha_1 = 0.02$, $\alpha_2 = 0.01$; (b) $\alpha_1 = 0$, $\alpha_2 = 0.001$.

shift Ω for $\alpha_2 = 0.01$ and $\alpha_2 = 0$. The results are shown in Fig. 4. We can see from Fig. 4(a) that the smaller absolute TOD will lead to the narrower pulse widths. This is consistent with the well-known experimental results from ultrashort pulse laser, so the compensation of TOD is very important in sub-100 fs mode-locked lasers. Fig. 4(b) shows the relationship between the inverse pulse widths and the slow variation part of loss α_1, it predicts that narrower pulses will occur for the smaller loss. From Fig. 4(c), we can recognize that smaller positive chirp will produce narrower pulses. And Fig. 4(d) predicts that narrower pulses will occur for the negative frequency shift than the positive frequency shift. These results are all consistent with the experimental observations in some mode-locked lasers and fiber amplifier systems [23–26].

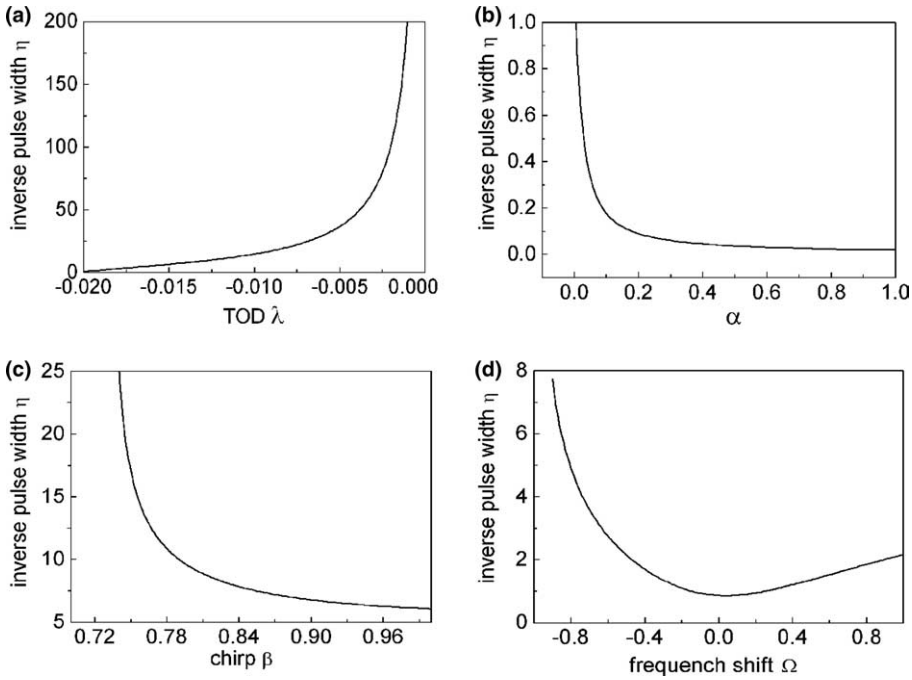

Fig. 4. The inverse pulse width η in dependence on typical parameters for $\alpha_1 = 0.01$, $\alpha_2 = 0$ (a) TOD λ; (b) absorption α_1; (c) chirp β; and (d) frequency shift Ω.

4. Stability

Since the parameter space is at least six-dimensional, the complete stability analysis of the solution is complicated both analytically and numerically. In order to analyze the stability of the pulses, we have made numerical evolutions of initial optical pulses under some perturbations (i.e., amplitude, chirp, and randomnoise) and the evolution of a quite arbitrary initial Gaussian pulse. The results show that the solution pulse is unstable when the parameters in Eq. (4), including δ, are fixed. In fact, any change of the amplitude of the pulse relative to the exact solution will change the total gain across the pulse, and the amplitude changes exponentially in the same direction. However, for a proper choice of the parameters, the pulse can become stable if the gain (or loss) $\delta = g - \delta_0$ depends on the total energy of the pulse, as shown in Eq. (2). The dependence of δ on the total energy Q serves as a feedback mechanism that stabilizes the pulse for a certain range of values of g_0, E_L, T_L, and δ_0.

Fig. 5 shows the pulse evolution under some perturbations with parameter values $\varepsilon = 0.13$, $\lambda = -0.02$, $\kappa = -0.03804$, $v = -0.01$, $D = 1$, $\delta = -0.01104$, $\chi = 0.07229$, $\alpha_1 = 0.02$, $\alpha_2 = 0.01$, $g_0 = 1$, $E_L = 10$, $T_L =;100$, and $T_R = 1$. Then the solution (5) has the parameters $\beta = 0.11512$, $\Omega = 0.00853$, $\eta = 0.76604$, $A_0 = 0.7803$, $K = -0.30675$, and $V = 0.02431$. The evolution of an initial pulse, which is $E(0,t) = 1.1A_0\mathrm{sech}(\eta t)\exp[\mathrm{i}(\Omega t + 0.5t^2)]$, is shown in Fig. 5(a). We can see that the initial pulse becomes stable and identical to the exact solution after 1000 round trips. Note that the initial chirp is different from that in the exact solution. This difference induces the abrupt changes in the beginning. Nevertheless, finally the solution approaches the exact one. Fig. 5(b) shows the evolution under the perturbation of white noise whose maximal value is 0.2. From the evolution behaviors of the pulses, we can conclude that the soliton-like solution is stable under finite initial perturbations (see also the inlays in Fig. 5(a)–(c), which show comparisons of pulses at typical distance z with the initial one as well as exact distributions). Finally, we investigated the evolution of a quite arbitrary Gaussian pulse $E(0,t) = \exp(-t^2)$, which

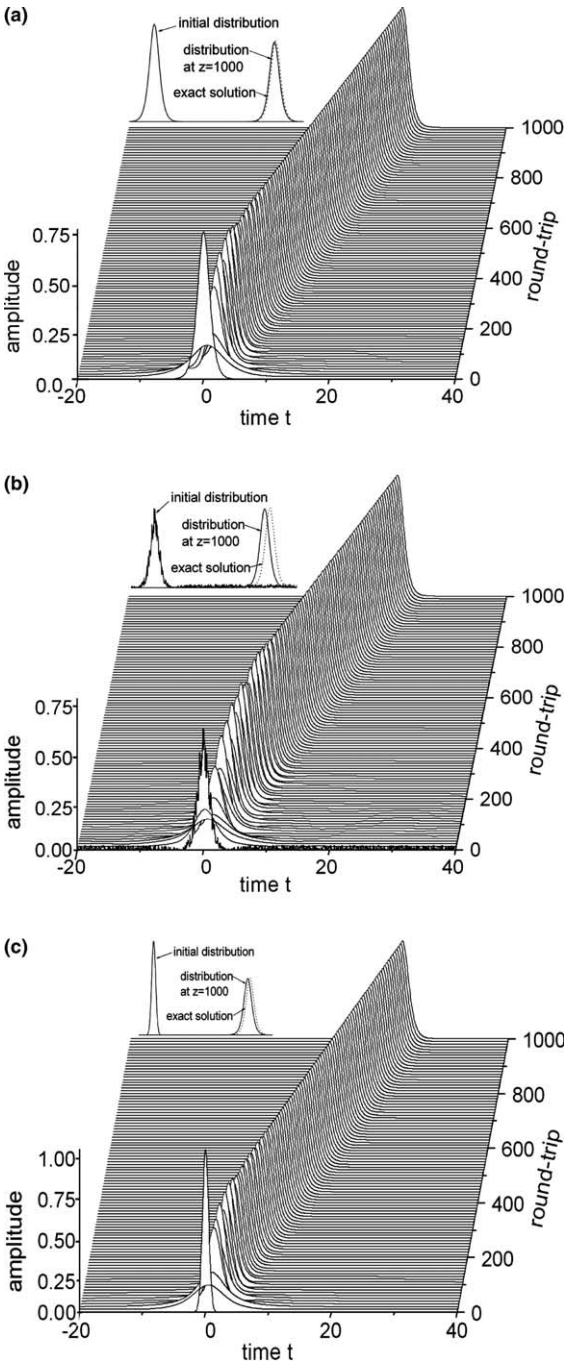

Fig. 5. Evolution of different initial pulse for $\alpha_1 = 0.02$, $\alpha_2 = 0.01$: (a) An initial pulse with perturbations in both amplitude and chirp. (b) An initial pulse under the perturbation of white noise whose maximal value is 0.2. (c) A quite arbitrary initial Gaussian pulse $E(0,t) = \exp(-t^2)$.

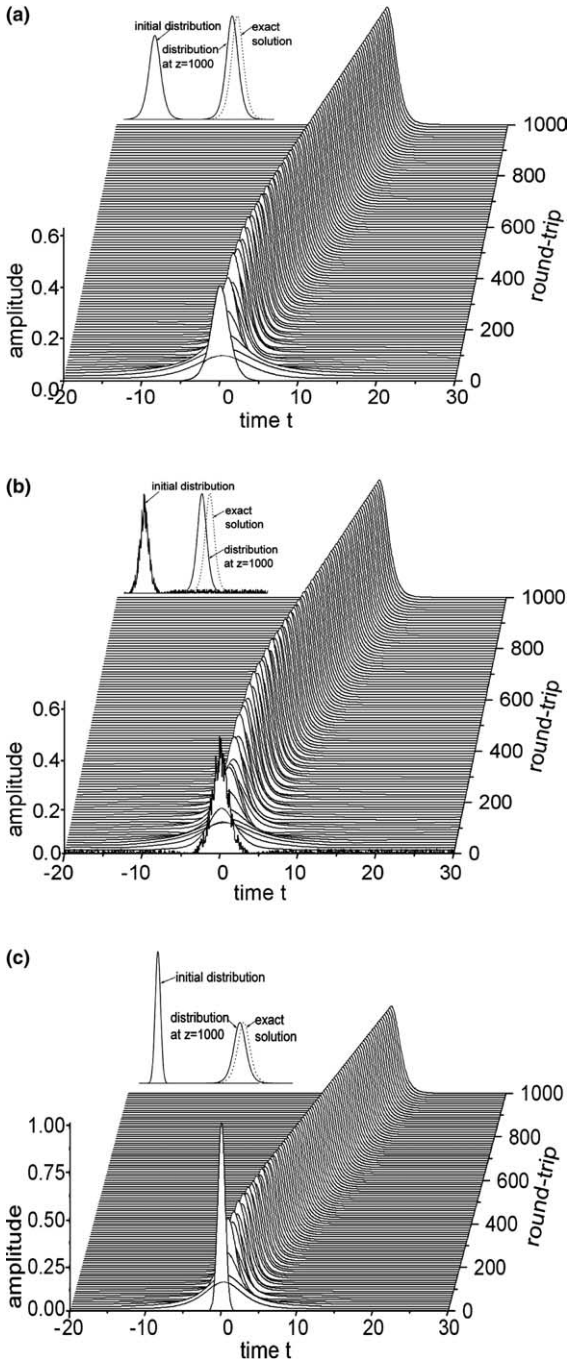

Fig. 6. Evolution of different initial pulse for $\alpha_1 = 0$, $\alpha_2 = 0.001$: (a) An initial pulse with perturbations in both amplitude and chirp. (b) An initial pulse under the perturbation of white noise whose maximal value is also equal to 0.2. (c) A quite arbitrary initial Gaussian pulse $E(0,t) = \exp(-t^2)$.

was shown in Fig. 5(c). It shows that the initial Gaussian pulse converges to the exact solution after a distance of evolution. The evolutions of the solution for $\alpha_1 = 0$, $\alpha_2 = 0.001$ are shown in Fig. 6(a)–(c), in which the equation parameters values are the same as Fig. 5. Fig. 6(a) shows the evolution of the initial pulse under the perturbations in amplitude and chirp, which is $E(0,t) = 0.9A_0\mathrm{sech}(\eta t)\exp[\mathrm{i}(\Omega t + 0.3\mathrm{t}^2)]$ and Ω, η, and A_0 have the values of the exact solution presented above. We can see that, when the absorption coefficient $\alpha_1 \to 0$ and the quadratic in energy term is taken into account, the soliton-like solution is also stable under the feedback mechanism caused by the dependence of δ on the total energy Q. Then, we analyze the evolution of an initial pulse under the perturbation of white noise, whose maximal value is also equal to 0.2, and a quite arbitrary Gaussian pulse. As shown in Fig. 6(b) and (c), the pulses became identical to the exact solution after a distance of evolution.

5. Conclusion

In conclusion, we have obtained analytically the soliton-like solution for a higher-order complex Ginzberg–Landau equation, which includes the saturable-absorber responses and higher-order effects, such as TOD, nonlinear dispersion, and self-frequency shift arising from stimulated Raman scattering. We have also analyzed the dependence of the inverse pulse width η on the TOD λ, the slow variation of loss α_1, the chirp parameter β and the frequency shift Ω. The stability of the soliton-like pulse under some perturbations (i.e., amplitude, chirp, and white noise) is analyzed numerically. The results show that the pulses can become stable for a proper choice of the initial parameters, in which the feedback mechanism of the loss (or gain) plays an important role in stabilizing the soliton. In addition, we have also considered the evolution of a quite arbitrary initial Gaussian pulse and found that it is gradually converged to the analytically exact solution after a distance of evolution. All of these results show that stable soliton-like pulses can be generated by passively mode-locking lasers, in which the combined

balances among the high-order effects, saturable absorber responses and other effects presented in the equation finish the pulses formation and stabilization.

Acknowledgements

The authors are grateful for the insightful suggestions from the anonymous referees. This work is supported by the National Natural Science Foundation of China, Grant No. 60477026, and the Provincial Overseas Scholar Foundation of Shanxi. The permanent corresponding address is zhougs@sxu.edu.cn.

References

[1] U. Keller, D.A.B. Miller, G.D. Boyd, T.H. Chiu, J.F. Ferguson, M.T. Asom, Opt. Lett. 17 (1992) 505.
[2] Y.P. Tong, P.M.W. French, J.R. Taylor, J.O. Fujimoto, Opt. Commun. 136 (1997) 235.
[3] M.J. Hayduk, S.T. Johns, M.F. Krol, C.R. Pollock, R.P. Leavitt, Opt. Commun. 137 (1997) 55.
[4] Z. Zhang, T. Nakagawa, K. Torizuka, T. Sugaya, K. Kobayashi, Appl. Phys. B 70 (2000) S59.
[5] A.A. Lagatsky, C.G. Leburn, C.T.A. Brown, W. Sibbett, W.H. Knox, Opt. Commun. 217 (2003) 363.
[6] H.A. Haus, J. Appl. Phys. 46 (1975) 3049.
[7] V.L. Kalashnikov, D.O. Krimer, I.G. Poloyko, V.P. Mikhailov, Opt. Commun. 159 (1999) 237.
[8] V.L. Kalashnikov, Opt. Commun. 192 (2001) 323.
[9] Z. Li, L. Li, H. Tian, G. Zhou, K.H. Spatschek, Phys. Rev. Lett. 89 (2002) 263901.
[10] N.N. Akhmediev, A. Ankiewicz, M.J. Lederer, B. Luther-Davies, Opt. Lett. 23 (1998) 280.
[11] R. Ell, U. Morgner, F.X. Krtner, J.G. Fujimoto, E.P. Ippen, V. Scheuer, G. Angelow, T. Tschudi, M.J. Lederer, A. Boiko, B. Luther-Davies, Opt. Lett. 26 (2001) 373.
[12] P.C. Wagenblast, U. Morgner, F. Grawert, T.R. Schibli, F.X. Krtner, V. Scheuer, G. Angelow, M.J. Lederer, Opt. Lett. 27 (2002) 1726.
[13] P. Wagenblast, R. Ell, U. Morgner, F. Grawert, F.X. Krtner, Opt. Lett. 28 (2003) 1713.
[14] K. Yamane, Z. Zhang, K. Oka, R. Morita, M. Yamashita, A. Suguro, Opt. Lett. 28 (2003) 2258.
[15] M.J. Lederer, B. Luther-Davies, H.H. Tan, C. Jagadish, Appl. Phys. Lett. 70 (1997) 3428.
[16] U. Keller, K.J. Weingarter, F.X. Kartner, D. Kopf, B. Braun, I.D. Jung, R. Fluck, C. Honninger, N. Mauschek, J.A. der Au, IEEE J. Sel. Top. Quantum Electron. 2 (1996) 435.
[17] G.H.C. New, Opt. Commun. 6 (1974) 188.
[18] H.A. Haus, IEEE J. Quantum Electron. 11 (1975) 736.
[19] H.A. Haus, J.G. Fujimoto, E.P. Ippen, J. Opt. Soc. Am. B 8 (1991) 2068.
[20] F.X. Kartner, U. Keller, Opt. Lett. 20 (1995) 16.
[21] I.D. Jung, F.X. Kartner, L.R. Brovelli, M. Kamp, U. Keller, Opt. Lett. 20 (1995) 1892.
[22] F.X. Kartner, I.D. Jung, U. Keller, IEEE J. Sel. Topics Quantum Electron. 2 (1996) 540.
[23] I.T. Sorokina, E. Sorokin, E. Wintner, A. Cassanho, H.P. Jenssen, R. Szipöcs, Opt. Lett. 22 (1997) 1716.
[24] M. Nakazawa, K. Kurokawa, H. Kubota, K. Suzuki, Y. Kimura, Appl. Phys. Lett. 57 (1990) 653.
[25] K. Kurokawa, M. Nakazawa, Appl. Phys. Lett. 58 (1991) 2871.
[26] S. Naumov, E. Sorokin, V.L. Kalashnikov, G. Tempea, I.T. Sorokina, Appl. Phys. B 76 (2003) 1.